Shape Preserving Positive and Convex Data Visualization using Rational Bi-cubic Functions

[1]Muhammad Sarfraz, [2]Malik Zawwar Hussain, [3]Tahira Sumbal Shaikh

[1]Department of Information Science, Adailiya Campus, Kuwait University, Kuwait
E-mail: prof.m.sarfraz@gmail.com

[2, 3]Department of Mathematics, University of the Punjab, Lahore, Pakistan

E-mail: malikzawwar.math@pu.edu.pk

Abstract

This paper is concerned with the problem of positive and convex data visualization in the form of positive and convex surfaces. A rational bi-cubic partially blended function with eight free parameters in its description is introduced and applied to visualize the shape of positive data and convex data. The developed schemes in this paper have unique representations. Visual models of surfaces attain C^1 smoothness.

Keywords: Data visualization; rational cubic function; rational bi-cubic partially blended function; positive surface; convex surface.

1. Introduction

Splines are basic tools for the visualization of the shaped data. Although ordinary splines smoothly interpolate the given data points but do not fulfill the hidden shape properties of the data. Dealing with different shapes (like monotony, positivity. or convexity), data visualization has significant role for various real life applications. This paper specifically concentrates on the visualization of positive and convex data in the form of surfaces.

There are many fields where the entities only have meaning when their values are positive. For instance, in probability distributions, the representation of data is always positive. Similarly, when we deal with the samples of populations, the data are always in positive figures. Convexity is also an important shape feature and plays a significant role in various disciplines and applications. For example, nonlinear programming in engineering, scientific applications such as design, optimal control, parameter estimation and approximation of functions are few of them to mention. One can observe that in Figure 1, bi-cubic Hermite function interpolates the positive data but inherent shape feature (i.e. positivity) is missing in the resultant surface representation. Similarly in Figure 7, bi-cubic Hermite function interpolates the convex data but inherent shape feature (i.e. convexity) is lost in the ultimate surface representation. This motivates to come up with the schemes which can preserve the inherent features of the data.

In recent years, researchers [1-16] have published a significant number of articles in the field of shape persevering data visualization. Asim and Brodlie [1] discussed the problem of drawing positive curve through positive data. A piecewise cubic Hermite interpolation is used to fit a positive curve. In any interval where the positivity is lost authors added extra knots to cubic Hermite interpolant to obtain desired positive curve. Brodlie et al [2] adopted modified quadratic Shepard (MQS) method for the interpolation of scattered data of any dimension. They restricted the range of interpolating function between 0 and 1. Positivity of positive scattered data is achieved by MQS method but the graphical results are not visually pleasant. Brodlie et al [3] presented an algorithm for the visualization of positive data. They derived sufficient conditions in terms of first partial derivatives and mixed partial derivatives at the grid points. They also generalized the case of linearly constrained interpolation. Casciola and Romani [4] constructed NURBS with tension parameters to control the shape of interpolatory surfaces. They presented some techniques to reconstruct the shape preserving bivariate NURBS, in which shapes of resulting surfaces can be modified by changing the values of tension parameters. Duan et al [5] constructed a bivariate rational interpolating function based on the function values and partial derivatives. They attached six parameters in the description of bivariate interpolating function to keep the interpolating surface in the original shape. Fangxum et al [6] presented an explicit expression of a weighted blending interpolator based on the function values. In [6] positive parameters and weight coefficients are freely selected according to the needs of practical design and the interpolator is C^1 in the whole interpolating region. Fujisawa et al [7] briefly described the implementation and visualization through some examples of applications to scientific arts such as archeology, sculpture, fine arts and information aesthetics. Hussain et al [8, 9] discussed visualization of 3D convex data. In [8] they used rational bi-cubic function while in [9] they used rational bi-quartic function to visualize convex data. They imposed conditions on free parameters in the description of rational functions to visualize convex data.

Kouibia and Pasadas [11] presented an approximation problem of parametric curves and surfaces from the Lagrange or Hermite data set. They also discussed the interpolation problem of minimizing some functional on a Sobolev space that produced the new notion of interpolating variational spline. Piah et al [12] presented two algorithms for the positivity preservation of scattered data. The interpolating surface comprises cubic Bezier triangular patches with sufficient conditions imposed on the ordinates of the Bazier control points in each triangle to guarantee preservation of positivity. Renka [13] discussed the construction of C^1 convex surface interpolation. For this purpose Renka introduced a Fortran-77 software package. Sarfraz et al [14] constructed a rational cubic function with two parameters in its representation and extended the rational cubic function to rational bi-cubic partially blended function. They visualized the shape of positive data in the form of positive curves and surfaces by introducing constraints on parameters. Wang and Tan [15] generated a rational bi-quartic surface by using tensor product method. They developed an algorithm to preserve the shape of monotone data by piecewise rational bi-quartic function. Zhang et al [16] dealt out the problem of convexity control of interpolating bivariate surfaces. Sufficient and necessary conditions are derived to obtain convex surface through convex data based on the function values.

In this paper, a rational bi-cubic function is used to visualize the shaped data. Two schemes are developed; one for the surface visualization of positive data and the other for the surface visualization of convex data. Important features of this paper are as follows:

- Developed schemes are designed in such a way that no additional knots are necessary to control the shape as in [1].
- There is no limitation on the interpolating function for lying in a specified interval as in [2].
- In this paper constraints are derived on free parameters which provide more control to the user to control the shape of interpolating surface as compared to the scheme in [3].
- Developed schemes are equally applicable for the data with derivative or without derivatives while schemes in [4, 5] developed the work if partial derivatives at the knots are known.
- In [9] rational bi-quartic function is used to preserve the shape of convex surface data while in this paper we used rational bi-cubic function to visualize the convex surface data.
- In [14] authors claimed that positive surfaces generated by their schemes are C^1 continuous and smooth. Similarly, the surfaces generated by the proposed schemes developed in this paper are also C^1 continuous.
- Developed schemes are useful for both equally spaced as well as unequally spaced data while in [15] authors derived results for equally spaced data.
- Generated surfaces are unique in their representation.

This paper is organized as follows. Section 2 is a review of curve interpolant of [10]. Section 3 deals with the piecewise rational bi-cubic partially blended function. Sections 4 and 5 deal with the tasks of visualization for positive and convex data respectively. Section 6 concludes the paper.

2. Rational Cubic Function

Let $\{(x_i, f_i),\ i = 1, 2, 3, \dots, n\}$ be given set of data points where $x_1 < x_2 < \dots < x_n$. In each interval $[x_i, x_{i+1}]$, the rational cubic function $S(x)$ is defined as:

$$S(x) \equiv S(x_i) = \frac{\mu_i U_i (1-\theta)^3 + W_i \theta (1-\theta)^2 + T_i \theta^2 (1-\theta) + \upsilon_i V_i \theta^3}{\mu_i (1-\theta)^2 + (\mu_i + \upsilon_i)\theta(1-\theta) + \upsilon_i \theta^2} \qquad (1)$$

where

$U_i = f_i$,

$W_i = \mu_i h_i d_i + (2\mu_i + \upsilon_i) f_i$,

$T_i = -\upsilon_i h_i d_{i+1} + (\mu_i + 2\upsilon_i) f_{i+1}$,

$V_i = f_{i+1}$,

and $\theta = \frac{x - x_i}{h_i}$, $h_i = x_{i+1} - x_i$, $\forall\ i = 1, 2, 3, \ldots, n-1$.

The rational cubic function (1) has following properties:

$$\left.\begin{array}{ll} S(x_i) = f_i, & S(x_{i+1}) = f_{i+1}, \\ S^{(1)}(x_i) = d_i, & S^{(1)}(x_{i+1}) = d_{i+1} \end{array}\right\} \tag{2}$$

where $S^{(1)}(x_i)$ denote the first order derivative with respect to x and d_i denotes derivative value at the knot x_i.

Remark: It is observed that when $\mu_i = \upsilon_i = 1$ the rational cubic function (1) reduces to the standard cubic Hermite polynomial $S(x) \in C^1[x_1, x_n]$.

Following Theorems 1 and 2 follow from [10]:

Theorem 1: The rational cubic function (1) is positive in each interval $[x_i, x_{i+1}]$ if the shape parameters μ_i, υ_i satisfy the following constraints:

$$\upsilon_i > 0,$$

$$\mu_i = \kappa_i + \max\left\{0, \frac{-\upsilon_i f_i}{2 f_i + h_i d_i}, \frac{(h_i d_{i+1} - 2 f_i)\upsilon_i}{f_{i+1}}\right\}, \qquad \kappa_i > 0.$$

Theorem 2: The rational cubic function (1) is convex in each interval $[x_i, x_{i+1}]$ if the shape parameters μ_i, υ_i satisfy the following constraints:

$$\upsilon_i > 0,$$

$$\mu_i = \delta_i + \max\left\{0, \frac{(d_{i+1} - d_i)\upsilon_i}{(\Delta_i - d_i)}, \frac{(\Delta_i - d_{i+1})\upsilon_i}{(d_i - \Delta_i)}\right\}, \quad \delta_i > 0.$$

3. Rational Bi-cubic Function

A piecewise rational cubic function (1) is extended to rational bi-cubic partially blended function $S(x, y)$ over the rectangular region $\Omega = [a,b] \times [c,d]$. Let $\pi : a = x_0 < x_1 < \ldots < x_n = b$ be partition of $[a,b]$ and $\tilde{\pi} : c = y_0 < y_1 < \ldots < y_m = d$ be the partition of $[c,d]$, the rational bi-cubic partially blended function is defined over each rectangular patch $[x_i, x_{i+1}] \times [y_j, y_{j+1}]$, $i = 0, 1, 2, \ldots, n-1$; $j = 0, 1, 2, \ldots, m-1$ as:

$$S(x,y) = -PFQ^T \tag{3}$$

where

$$F = \begin{pmatrix} 0 & S(x,y_j) & S(x,y_{j+1}) \\ S(x_i,y) & S(x_i,y_j) & S(x_i,y_{j+1}) \\ S(x_{i+1},y) & S(x_{i+1},y_j) & S(x_{i+1},y_{j+1}) \end{pmatrix},$$

$$P = \begin{bmatrix} -1 & p_0(\theta) & p_1(\theta) \end{bmatrix},\ Q = \begin{bmatrix} -1 & q_0(\phi) & q_1(\phi) \end{bmatrix},$$

with $p_0 = (1-\theta)^2(1+2\theta),\ p_1 = \theta^3(3-2\theta),\ q_0 = (1-\phi)^2(1+2\phi),\ q_1 = \phi^2(3-2\phi)$.

$\theta = (x-x_i)/h_i$, $h_i = x_{i+1}-x_i$, $\phi = (y-y_j)/\hat{h}_j$, $\hat{h}_j = y_{j+1}-y_j$, $0 \le \theta,\phi \le 1$.

$S(x,y_j)$, $S(x,y_{j+1})$, $S(x_i,y)$ and $S(x_{i+1},y)$ are rational cubic function (1) defined over the boundary of rectangular patch $[x_i,x_{i+1}]\times[y_j,y_{j+1}]$ as:

$$S(x,y_j) = \frac{\sum_{i=1}^{4} A_{i,j}(1-\theta)^{4-i}\theta^{i-1}}{q_{i,j}(\theta)} \tag{4}$$

with

$A_{1,j} = \mu_{i,j}^2 F_{i,j}$,

$A_{2,j} = (2\mu_{i,j}+\upsilon_{i,j})F_{i,j} + \mu_{i,j}h_i F_{i,j}^x$,

$A_{3,j} = (\mu_{i,j}+2\upsilon_{i,j})F_{i+1,j} - \upsilon_{i,j}h_i F_{i+1,j}^x$,

$A_{4,j} = \upsilon_{i,j}^2 F_{i+1,j}$,

$q_{i,j}(\theta) = \mu_{i,j}(1-\theta)^2 + (\mu_{i,j}+\upsilon_{i,j})\theta(1-\theta) + \upsilon_{i,j}\theta^2$,

$$S(x,y_{j+1}) = \frac{\sum_{i=1}^{4} B_{i,j}(1-\theta)^{4-i}\theta^{i-1}}{q_{i,j+1}(\theta)} \tag{5}$$

with

$B_{1,j} = \mu_{i,j+1}^2 F_{i,j+1}$,

$B_{2,j} = (2\mu_{i,j+1}+\upsilon_{i,j+1})F_{i,j+1} + \mu_{i,j+1}h_i F_{i,j+1}^x$,

$B_{3,j} = (\mu_{i,j+1}+2\upsilon_{i,j+1})F_{i+1,j+1} - \upsilon_{i,j+1}h_i F_{i+1,j+1}^x$,

$B_{4,j} = \upsilon_{i,j+1}^2 F_{i+1,j}$,

$q_{i,j+1}(\theta) = \mu_{i,j+1}(1-\theta)^2 + (\mu_{i,j+1}+\upsilon_{i,j+1})\theta(1-\theta) + \upsilon_{i,j+1}\theta^2$,

$$S\left(x_i, y\right) = \frac{\sum_{i=1}^{4} C_{i,j}\left(1-\phi\right)^{4-i}\phi^{i-1}}{\hat{q}_{i,j}\left(\phi\right)} \tag{6}$$

with

$C_{1,j} = \hat{\mu}_{i,j}^2 F_{i,j}$,

$C_{2,j} = \left(2\hat{\mu}_{i,j} + \hat{\upsilon}_{i,j}\right)F_{i,j} + \hat{\mu}_{i,j}\hat{h}_j F_{i,j}^y$,

$C_{3,j} = \left(\hat{\mu}_{i,j} + 2\hat{\upsilon}_{i,j}\right)F_{i,j+1} - \hat{\upsilon}_{i,j}\hat{h}_j F_{i,j+1}^y$,

$C_{4,j} = \hat{\upsilon}_{i,j}^2 F_{i,j+1}$,

$\hat{q}_{i,j}\left(\phi\right) = \hat{\mu}_{i,j}\left(1-\phi\right)^2 + \left(\hat{\mu}_{i,j} + \hat{\upsilon}_{i,j}\right)\phi\left(1-\phi\right) + \hat{\upsilon}_{i,j}\phi^2$,

$$S\left(x_{i+1}, y\right) = \frac{\sum_{i=1}^{4} D_{i,j}\left(1-\phi\right)^{4-i}\phi^{i-1}}{\hat{q}_{i+1,j}\left(\phi\right)} \tag{7}$$

with

$D_{1,j} = \hat{\mu}_{i+1,j}^2 F_{i,j}$,

$D_{2,j} = \left(2\hat{\mu}_{i+1,j} + \hat{\upsilon}_{i+1,j}\right)F_{i+1,j} + \hat{\mu}_{i+1,j}\hat{h}_j F_{i+1,j}^y$,

$D_{3,j} = \left(\hat{\mu}_{i+1,j} + 2\hat{\upsilon}_{i+1,j}\right)F_{i+1,j+1} - \hat{\upsilon}_{i+1,j}\hat{h}_j F_{i+1,j+1}^y$,

$D_{4,j} = \hat{\upsilon}_{i+1,j}^2 F_{i+1,j+1}$,

$\hat{q}_{i+1,j}\left(\phi\right) = \hat{\mu}_{i+1,j}\left(1-\phi\right)^2 + \left(\hat{\mu}_{i+1,j} + \hat{\upsilon}_{i+1,j}\right)\phi\left(1-\phi\right) + \hat{\upsilon}_{i+1,j}\phi^2$.

3.1. Choice of Derivatives

For most of the applications, the derivative parameters are unknown. There are many methods for the approximation of these derivative parameters. In this article, they are calculated by Arithmetic Mean Method. The description of this method is as follows. Let $F_{i,j}^x$ and $F_{i,j}^y$ denote the first derivative with respect to x and y respectively and $F_{i,j}^{xy}$ be the mixed derivative at the data point $F_{i,j}$.

$F_{0,j}^x = \hat{\Delta}_{0,j} + \frac{\left(\hat{\Delta}_{0,j} - \hat{\Delta}_{1,j}\right)h_0}{\left(h_0 + h_1\right)}$,

$F_{m,j}^x = \hat{\Delta}_{m-1,j} + \frac{\left(\hat{\Delta}_{m-1,j} - \hat{\Delta}_{m-2,j}\right)h_{m-1}}{h_{m-1} + h_{m-2}}$,

$F_{i,j}^x = \frac{\Delta_{i,j} - \Delta_{i-1,j}}{2}$, $i = 1, 2, ..., m-1;\ j = 0, 1, 2, ..., n$

$F_{i,n}^y = \hat{\Delta}_{i,n-1} + \frac{\left(\hat{\Delta}_{i,n-1} - \hat{\Delta}_{i,n-2}\right)\hat{h}_{n-1}}{\hat{h}_{n-1} + \hat{h}_{n-2}}$,

$$F_{i,j}^{y}=\frac{\hat{\Delta}_{i,j}-\hat{\Delta}_{i,j-1}}{2}, \qquad i=0,1,2,...,m;\ j=1,2,...,n-1$$

$$F_{i,j}^{xy}=\frac{1}{2}\left\{\frac{F_{i,j+1}^{x}-F_{i,j-1}^{x}}{\hat{h}_{j-1}+\hat{h}_{j}}+\frac{F_{i+1,j}^{x}-F_{i-1,j}^{x}}{h_{i-1}+h_{i}}\right\}, \qquad i=1,2,...,m-1;\ j=1,2,...,n-1$$

$$\Delta_{i,j}=\frac{F_{i+1,j}-F_{i,j}}{h_i},\ \ \hat{\Delta}_{i,j}=\frac{F_{i,j+1}-F_{i,j}}{\hat{h}_j}.$$

4. Positive Rational Bi-cubic Function

Let $\left\{\left(x_i, y_j, F_{i,j}\right): i=0,1,2,...,n\ ;\ j=0,1,2,...,m\right\}$ be the set of positive data points defined over rectangular grid $I_{i,j}=\left[x_i,x_{i+1}\right]\times\left[y_j,y_{j+1}\right]$, $i=0,1,2,...,n-1$; $j=0,1,2,...,m-1$. Due to Casciola and Romani [4], bi-cubic partially blended surface patch inherits all the properties of network of boundary curves. Therefore, bi-cubic partially blended surface patch defined in (3) will be positive in each rectangular patch $I_{i,j}=\left[x_i,x_{i+1}\right]\times\left[y_j,y_{j+1}\right]$, if each of the boundary curves $S\left(x,y_j\right)$, $S\left(x,y_{j+1}\right)$, $S\left(x_i,y\right)$ and $S\left(x_{i+1},y\right)$, is positive. Now the curves

$$S\left(x,y_j\right)>0 \text{ if } \upsilon_{i,j}>0,\ \mu_{i,j}>0,\ \mu_{i,j}>\frac{-\upsilon_{i,j}F_{i,j}}{2F_{i,j}+h_iF_{i,j}^{x}} \text{ and } \mu_{i,j}>\frac{\left(h_iF_{i+1,j}^{x}-2F_{i,j}\right)\upsilon_{i,j}}{F_{i+1,j}}$$

$$S\left(x,y_{j+1}\right)>0 \text{ if } \upsilon_{i,j+1}>0,\ \mu_{i,j+1}>0,\ \mu_{i,j+1}>\frac{-\upsilon_{i,j+1}F_{i,j+1}}{2F_{i,j+1}+h_iF_{i,j+1}^{x}} \text{ and } \mu_{i,j+1}>\frac{\left(h_iF_{i+1,j+1}^{x}-2F_{i,j+1}\right)\upsilon_{i,j+1}}{F_{i+1,j+1}}$$

$$S\left(x_i,y\right)>0 \text{ if } \hat{\upsilon}_{i,j}>0,\ \hat{\mu}_{i,j}>0,\ \hat{\mu}_{i,j}>\frac{-\hat{\upsilon}_{i,j}F_{i,j}}{2F_{i,j}+\hat{h}_jF_{i,j}^{y}} \text{ and } \hat{\mu}_{i,j}>\frac{\left(\hat{h}_jF_{i,j+1}^{y}-2F_{i,j}\right)\hat{\upsilon}_{i,j}}{F_{i,j+1}}$$

$$S\left(x_{i+1},y\right)>0 \text{ if } \hat{\upsilon}_{i+1,j}>0,\ \hat{\mu}_{i+1,j}>0,\ \hat{\mu}_{i+1,j}>\frac{-\hat{\upsilon}_{i+1,j}F_{i+1,j}}{2F_{i+1,j}+\hat{h}_jF_{i+1,j}^{y}} \text{ and } \hat{\mu}_{i+1,j}>\frac{\left(\hat{h}_jF_{i+1,j+1}^{y}-2F_{i+1,j}\right)\hat{\upsilon}_{i+1,j}}{F_{i+1,j+1}}.$$

All the above discussion can be summarized as:

Theorem 3: The rational bi-cubic partially blended function defined in (3) visualizes positive surface data in the view of positive surface in each rectangular patch $I_{i,j}=\left[x_i,x_{i+1}\right]\times\left[y_j,y_{j+1}\right]$, if the shape parameters $\mu_{i,j},\upsilon_{i,j},\mu_{i,j+1},\upsilon_{i,j+1},\hat{\mu}_{i,j},\hat{\upsilon}_{i,j},\hat{\mu}_{i+1,j}$ and $\hat{\upsilon}_{i+1,j}$ satisfy the following conditions:

$\upsilon_{i,j}>0$, $\upsilon_{i,j+1}>0$, $\hat{\upsilon}_{i,j}>0$, $\hat{\upsilon}_{i+1,j}>0$,

$$\mu_{i,j} = \delta_{i,j} + \max\left\{0,\ \frac{-\upsilon_{i,j}F_{i,j}}{2F_{i,j} + h_i F^x_{i,j}},\ \frac{\left(h_i F^x_{i+1,j} - 2F_{i,j}\right)\upsilon_{i,j}}{F_{i+1,j}}\right\}$$

$$\mu_{i,j+1} = \eta_{i,j} + \max\left\{0,\ \frac{-\upsilon_{i,j+1}F_{i,j+1}}{2F_{i,j+1} + h_i F^x_{i,j+1}},\ \frac{\left(h_i F^x_{i+1,j+1} - 2F_{i,j+1}\right)\upsilon_{i,j+1}}{F_{i+1,j+1}}\right\}$$

$$\hat{\mu}_{i,j} = \hat{\delta}_{i,j} + \max\left\{0,\ \frac{-\hat{\upsilon}_{i,j}F_{i,j}}{2F_{i,j} + \hat{h}_j F^y_{i,j}},\ \frac{\left(\hat{h}_j F^y_{i,j+1} - 2F_{i,j}\right)\hat{\upsilon}_{i,j}}{F_{i,j+1}}\right\}$$

$$\hat{\mu}_{i+1,j} = \hat{\eta}_{i,j} + \max\left\{0,\ \frac{-\hat{\upsilon}_{i+1,j}F_{i+1,j}}{2F_{i+1,j} + \hat{h}_j F^y_{i+1,j}},\ \frac{\left(\hat{h}_j F^y_{i+1,j+1} - 2F_{i+1,j}\right)\hat{\upsilon}_{i+1,j}}{F_{i+1,j+1}}\right\},$$

where $\delta_{i,j},\ \eta_{i,j},\ \hat{\delta}_{i,j},\ \hat{\eta}_{i,j} > 0$.

The above discussion can be summarized in the following algorithm for computation purposes:

Algorithm 1

Step 1. Enter the $(n+1)\times(m+1)$ positive data points $\left(x_i, y_j, F_{i,j}\right), i = 0,1,2,...,n;\ \ j = 0,1,2,...,m.$

Step 2. Estimate the derivatives $F^x_{i,j}, F^y_{i,j}$ and $F^{xy}_{i,j}$ at knots.

Step 3. Calculate the values of shape parameters $\mu_{i,j}, \upsilon_{i,j}, \mu_{i,j+1}, \upsilon_{i,j+1}, \hat{\mu}_{i,j}, \hat{\upsilon}_{i,j}, \hat{\mu}_{i+1,j}$ and $\hat{\upsilon}_{i+1,j}$ using Theorem 3.

Step 4. Substitute the values of $F_{i,j},\ F^x_{i,j}, F^y_{i,j}, F^{xy}_{i,j}$, $i = 0,1,2,...,n;\ j = 0,1,2,...,m$ and $\mu_{i,j}, \upsilon_{i,j}, \mu_{i,j+1}, \upsilon_{i,j+1}, \hat{\mu}_{i,j}, \hat{\upsilon}_{i,j}, \hat{\mu}_{i+1,j}$ and $\hat{\upsilon}_{i+1,j}$ $i = 0,1,2,...,n-1;\ \ j = 0,1,2,...,m-1$ in rational bi-cubic function (3) to obtain positive rational bi-cubic function.

Table 1. A data set generated by $F_1(x,y) = 0.0012 + \dfrac{1.25 + \cos(5.4y)}{6 + (3x-1)^2}$.

y_j / x_i	1	100	200	300
1	0.1897	0.0012	0.0012	0.0012
100	0.2200	0.0012	0.0012	0.0012
200	0.2022	0.0012	0.0012	0.0012
300	0.1749	0.0012	0.0012	0.0012

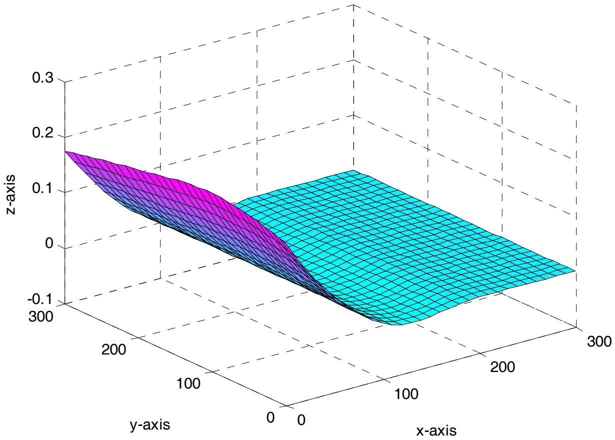

Figure 1. Bi-cubic Hermite Function

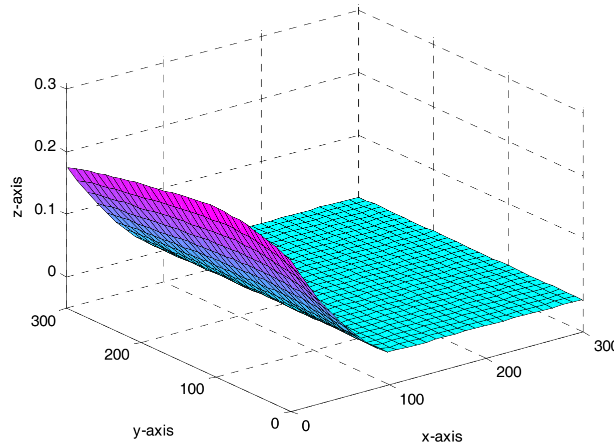

Figure 4. Positive rational bi-cubic Surface.

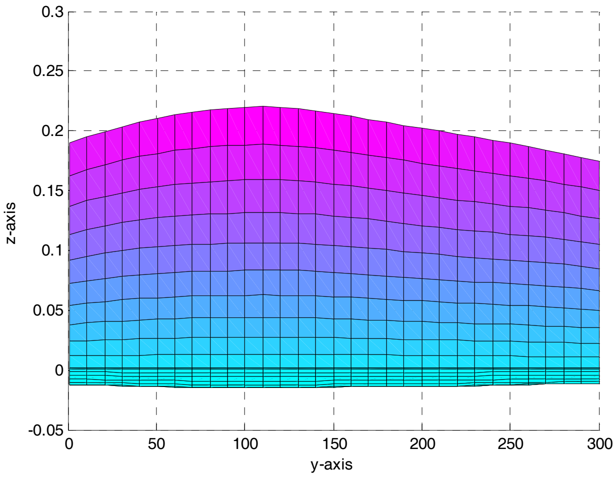

Figure 2. *yz*-view of Figure 1.

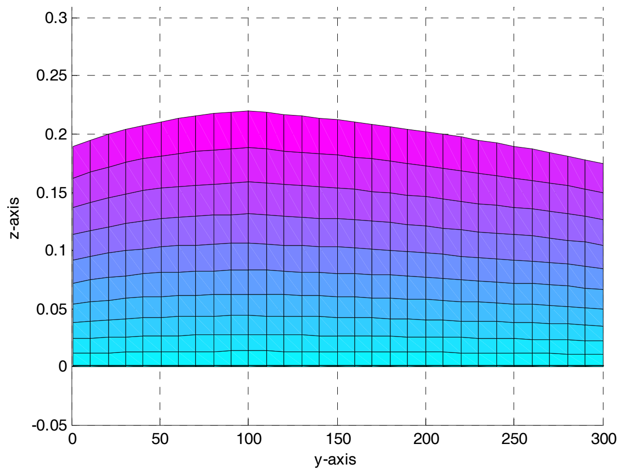

Figure 5. *yz*-view of Figure 4.

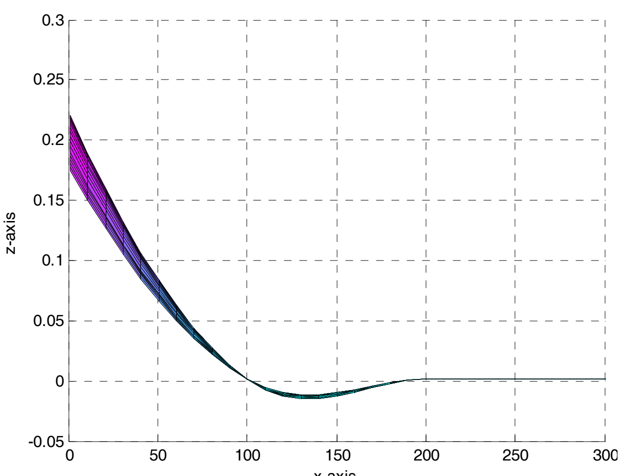

Figure 3. *xz*-view of Figure 1

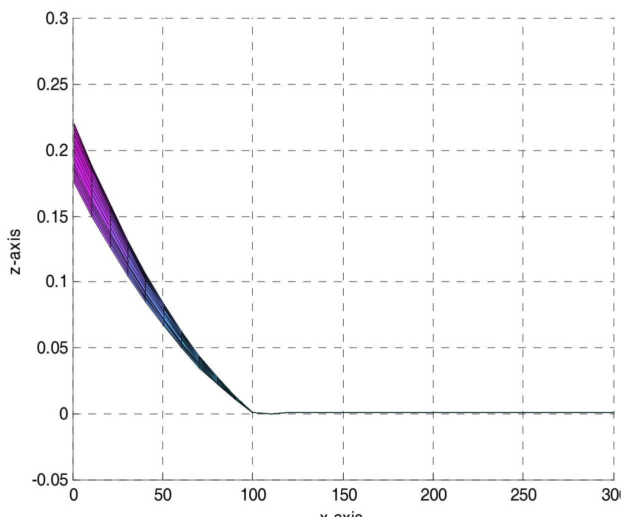

Figure 6. *xz*-view of Figure 4.

4.1. Demonstration:

A positive data set is taken in Table 1, which is generated by the function $F_1(x,y)=0.0012+\dfrac{1.25+\cos(5.4y)}{6+(3x-1)^2}$ correct to four decimal places defined over the rectangular grid $[1,300]\times[1,300]$. Figure 1 is generated using bi-cubic Hermite function, which interpolates the data points but does not visualize the shape of the data. Figures 2 and 3 are the *yz*-view and *xz*-view of Figure 1 respectively. Figure 4 is generated by the positive rational bi-cubic function developed in Section 4 with $\upsilon_{i,j}=\upsilon_{i,j+1}=\hat{\upsilon}_{i,j}=\hat{\upsilon}_{i+1,j}=0.5$. Figures 5 and 6 are the *yz*-view and *xz*-view of Figure 4 respectively. One can clearly observe that that Figure 4 preserves the shape of data taken in Table 1. The numerical results corresponding to the surface in Figure 4, for different parameters, are shown in Table 2. All the values in Table 2 are truncated up to four decimal places.

Table 2. Numerical results of Figure 4.

(x_i, y_j)	$F_x(i,j)$	$F_y(i,j)$	$\mu_{i,j}$	$\mu_{i,j+1}$	$\hat{\mu}_{i,j}$	$\hat{\mu}_{i+1,j}$
(1,1)	-0.0029	0.5475×10^{-3}	0.0025	0.0030	0.0040	0.0050
(1,100)	-0.0033	0.0641×10^{-3}	0.0025	0.0030	0.0040	0.0050
(1,200)	-0.0030	-0.2254×10^{-3}	0.0025	0.0030	0.0040	0.0050
(1,300)	-0.0026	-0.3195×10^{-3}	0.0025	0.0030	0.0040	0.0050
(100,1)	-0.0010	0.0001×10^{-3}	0.0025	0.0030	0.0040	0.0050
(100,100)	-0.0011	0.0000×10^{-3}	0.0025	0.0030	0.0040	0.0050
(100,200)	-0.0010	-0.0000×10^{-3}	0.0025	0.0030	0.0040	0.0050
(100,300)	-0.0009	-0.0000×10^{-3}	0.0025	0.0030	0.0040	0.0050
(200,1)	-0.0000	-0.0000×10^{-3}	0.0025	0.0030	0.0040	0.0050
(200,100)	-0.0000	-0.0000×10^{-3}	0.0025	0.0030	0.0040	0.0050
(200,200)	-0.0000	-0.0000×10^{-3}	0.0025	0.0030	0.0040	0.0050
(200,300)	-0.0000	-0.0000×10^{-3}	0.0025	0.0030	0.0040	0.0050
(300,1)	0.0000	-0.0000×10^{-3}	0.0025	0.0030	0.0040	0.0050
(300,100)	0.0000	-0.0000×10^{-3}	0.0025	0.0030	0.0040	0.0050
(300,200)	0.0000	-0.0000×10^{-3}	0.0025	0.0030	0.0040	0.0050
(300,300)	0.0000	-0.0000×10^{-3}	0.0025	0.0030	0.0040	0.0050

5. Convex Rational Bi-cubic Function

Let $\left\{\left(x_i, y_j, F_{i,j}\right): i=0,1,2,...,n\ ;\ j=0,1,2,...,m\right\}$ be the collection of convex data points defined over rectangular grid $I_{i,j}=\left[x_i, x_{i+1}\right]\times\left[y_j, y_{j+1}\right],\ \ i=0,1,2,...,n-1;\ \ j=0,1,2,...,m-1$. The data will be convex if it satisfies the following necessary conditions:

$$F_{i,j} < F_{i,j+1},\ \Delta_{i,j} > 0,\ F_{i,j} < F_{i+1,j},\ \hat{\Delta}_{i,j} > 0,\ F^x_{i,j} > 0,\ F^y_{i,j} > 0,$$
$$F^x_{i,j} < \Delta_{i,j} < F^x_{i+1,j},\ F^y_{i,j} < \hat{\Delta}_{i,j} < F^y_{i,j+1},\ F^x_{i,j} < F^x_{i+1,j},\ F^y_{i,j} < F^y_{i,j+1},\ \Delta_{i,j} < \Delta_{i+1,j},\ \hat{\Delta}_{i,j} < \hat{\Delta}_{i,j+1},\ \forall\ i,\ j$$

where

$$\Delta_{i,j} = \frac{F_{i+1,j} - F_{i,j}}{h_i},\ \ \hat{\Delta}_{i,j} = \frac{F_{i,j+1} - F_{i,j}}{\hat{h}_j}.$$

Due to Casciola and Romani [4], bi-cubic partially blended surface patch inherits all the properties of network of boundary curves. Therefore, the bi-cubic partially blended surface patch defined in (3) will be convex in each rectangular patch $I_{i,j} = [x_i, x_{i+1}] \times [y_j, y_{j+1}]$, if each of the boundary curves $S(x, y_j)$, $S(x, y_{j+1})$, $S(x_i, y)$ and $S(x_{i+1}, y)$ is convex i.e.

$$S^{(2)}(x, y_j) > 0,\ S^{(2)}(x, y_{j+1}) > 0,\ S^{(2)}(x_i, y) > 0 \text{ and } S^{(2)}(x_{i+1}, y) > 0\ \forall\ i, j.$$

The second ordered derivatives of the boundaries curves $S(x, y_j)$, $S(x, y_{j+1})$, $S(x_i, y)$ and $S(x_{i+1}, y)$ are as follows:

$$S^{(2)}(x, y_j) = \frac{\sum_{i=1}^{6} T_{i,j} \theta^{i-1} (1-\theta)^{6-i}}{\left(q_{i,j}(\theta)\right)^3} \tag{8}$$

where

$$T_{1,j} = 2\mu^2_{i,j} \left\{ \left(\mu_{i,j} + \upsilon_{i,j}\right)\left(\Delta_{i,j} - F^x_{i,j}\right) - \upsilon_{i,j}\left(F^x_{i+1,j} - \Delta_{i,j}\right) \right\} \Big/ h_i,$$
$$T_{2,j} = 2\upsilon^2_{i,j} \left\{ \left(2\mu_{i,j} + 5\upsilon_{i,j}\right)\left(\Delta_{i,j} - F^x_{i,j}\right) - 2\upsilon_{i,j}\left(F^x_{i+1,j} - \Delta_{i,j}\right) \right\} \Big/ h_i,$$
$$T_{3,j} = 2\mu_{i,j} \left\{ \mu_{i,j}\left(\mu_{i,j} + 7\upsilon_{i,j}\right)\left(\Delta_{i,j} - F^x_{i,j}\right) + \upsilon_{i,j}\left(F^x_{i+1,j} - \Delta_{i,j}\right)\left(-\mu_{i,j} + 3\upsilon_{i,j}\right) \right\} \Big/ h_i,$$
$$T_{4,j} = 2\upsilon_{i,j} \left\{ \mu_{i,j}\left(3\mu_{i,j} - \upsilon_{i,j}\right)\left(\Delta_{i,j} - F^x_{i,j}\right) + \upsilon_{i,j}\left(F^x_{i+1,j} - \Delta_{i,j}\right)\left(7\mu_{i,j} + \upsilon_{i,j}\right) \right\} \Big/ h_i,$$
$$T_{5,j} = 2\mu^2_{i,j} \left\{ \left(5\mu_{i,j} + 2\upsilon_{i,j}\right)\left(F^x_{i+1,j} - \Delta_{i,j}\right) - 2\upsilon_{i,j}\left(\Delta_{i,j} - F^x_{i,j}\right) \right\} \Big/ h_i,$$
$$T_{6,j} = 2\upsilon^2_{i,j} \left\{ \left(\mu_{i,j} + \upsilon_{i,j}\right)\left(F^x_{i+1,j} - \Delta_{i,j}\right) - \mu_{i,j}\left(\Delta_{i,j} - F^x_{i,j}\right) \right\} \Big/ h_i.$$

Similarly

$$S^{(2)}(x, y_j) > 0, \text{ if } T_{i,j}{}^{'}s > 0, \quad i = 1, 2, ..., 6 \text{ and } q_{i,j}(\theta) > 0$$

$q_{i,j}(\theta) > 0$ if $\mu_{i,j} > 0$, $\upsilon_{i,j} > 0$ and $T_{i,j}{}^{'}s > 0$, if

$$\mu_{i,j} > 0,\ \upsilon_{i,j} > 0,\ \mu_{i,j} > \frac{\left(F^x_{i+1,j} - F^x_{i,j}\right)\upsilon_{i,j}}{\left(\Delta_{i,j} - F^x_{i,j}\right)} \text{ and } \mu_{i,j} > \frac{\left(\Delta_{i,j} - F^x_{i+1,j}\right)\upsilon_{i,j}}{\left(\Delta_{i,j} - F^x_{i,j}\right)}$$

$$S^{(2)}\left(x, y_{j+1}\right) = \frac{\sum_{i=1}^{6} S_{i,j}\theta^{i-1}\left(1-\theta\right)^{6-i}}{\left(q_{i,j+1}\left(\theta\right)\right)^3} \tag{9}$$

where

$$S_{1,j} = 2\mu^2_{i,j+1}\left\{\left(\mu_{i,j+1} + \upsilon_{i,j+1}\right)\left(\Delta_{i,j+1} - F^x_{i,j+1}\right) - \upsilon_{i,j+1}\left(F^x_{i+1,j+1} - \Delta_{i,j+1}\right)\right\} \big/ h_i ,$$
$$S_{2,j} = 2\upsilon^2_{i,j+1}\left\{\left(2\mu_{i,j+1} + 5\upsilon_{i,j+1}\right)\left(\Delta_{i,j+1} - F^x_{i,j+1}\right) - 2\upsilon_{i,j+1}\left(F^x_{i+1,j+1} - \Delta_{i,j+1}\right)\right\} \big/ h_i ,$$
$$S_{3,j} = 2\mu_{i,j+1}\left\{\mu_{i,j+1}\left(\mu_{i,j+1} + 7\upsilon_{i,j+1}\right)\left(\Delta_{i,j+1} - F^x_{i,j+1}\right) + \upsilon_{i,j+1}\left(F^x_{i+1,j+1} - \Delta_{i,j+1}\right)\left(-\mu_{i,j+1} + 3\upsilon_{i,j+1}\right)\right\} \big/ h_i ,$$
$$S_{4,j} = 2\upsilon_{i,j+1}\left\{\mu_{i,j+1}\left(3\mu_{i,j+1} - \upsilon_{i,j+1}\right)\left(\Delta_{i,j+1} - F^x_{i,j+1}\right) + \upsilon_{i,j+1}\left(F^x_{i+1,j+1} - \Delta_{i,j+1}\right)\left(7\mu_{i,j+1} + \upsilon_{i,j+1}\right)\right\} \big/ h_i ,$$
$$S_{5,j} = 2\mu^2_{i,j+1}\left\{\left(5\mu_{i,j+1} + 2\upsilon_{i,j+1}\right)\left(F^x_{i+1,j+1} - \Delta_{i,j+1}\right) - 2\upsilon_{i,j+1}\left(\Delta_{i,j+1} - F^x_{i,j+1}\right)\right\} \big/ h_i ,$$
$$S_{6,j} = 2\upsilon^2_{i,j+1}\left\{\left(\mu_{i,j+1} + \upsilon_{i,j+1}\right)\left(F^x_{i+1,j+1} - \Delta_{i,j+1}\right) - \mu_{i,j+1}\left(\Delta_{i,j+1} - F^x_{i,j+1}\right)\right\} \big/ h_i ,$$

Similarly

$S^{(2)}\left(x, y_{j+1}\right) > 0$, if $S_{i,j}{}^{'}s > 0$, $i = 1, 2, ..., 6$ and $q_{i,j+1}(\theta) > 0$

$q_{i,j+1}(\theta) > 0$ if $\mu_{i,j+1} > 0$, $\upsilon_{i,j+1} > 0$ and $S_{i,j}{}^{'}s > 0$, if

$$\mu_{i,j+1} > 0,\ \upsilon_{i,j+1} > 0,\ \mu_{i,j+1} > \frac{\left(F^x_{i+1,j+1} - F^x_{i,j+1}\right)\upsilon_{i,j+1}}{\left(\Delta_{i,j+1} - F^x_{i,j+1}\right)} \text{ and } \mu_{i,j+1} > \frac{\left(\Delta_{i,j+1} - F^x_{i+1,j+1}\right)\upsilon_{i,j+1}}{\left(\Delta_{i,j+1} - F^x_{i,j+1}\right)}$$

$$S^{(2)}\left(x_i, y\right) = \frac{\sum_{i=1}^{6} U_{i,j}\phi^{i-1}\left(1-\phi\right)^{6-i}}{\left(\hat{q}_{i,j}\left(\phi\right)\right)^3} \tag{10}$$

where

$$U_{1,j} = 2\hat{\mu}^2_{i,j}\left\{\left(\hat{\mu}_{i,j} + \hat{\upsilon}_{i,j}\right)\left(\hat{\Delta}_{i,j} - F^y_{i,j}\right) - \hat{\upsilon}_{i,j}\left(F^y_{i,j+1} - \hat{\Delta}_{i,j}\right)\right\} \big/ \hat{h}_j ,$$
$$U_{2,j} = 2\hat{\upsilon}^2_{i,j}\left\{\left(2\hat{\mu}_{i,j} + 5\hat{\upsilon}_{i,j}\right)\left(\hat{\Delta}_{i,j} - F^y_{i,j}\right) - 2\hat{\upsilon}_{i,j}\left(F^y_{i,j+1} - \hat{\Delta}_{i,j}\right)\right\} \big/ \hat{h}_j ,$$
$$U_{3,j} = 2\hat{\mu}_{i,j}\left\{\hat{\mu}_{i,j}\left(\hat{\mu}_{i,j} + 7\hat{\upsilon}_{i,j}\right)\left(\hat{\Delta}_{i,j} - F^y_{i,j}\right) + \hat{\upsilon}_{i,j}\left(F^y_{i,j+1} - \hat{\Delta}_{i,j}\right)\left(-\hat{\mu}_{i,j} + 3\hat{\upsilon}_{i,j}\right)\right\} \big/ \hat{h}_j ,$$
$$U_{4,j} = 2\hat{\upsilon}_{i,j}\left\{\hat{\mu}_{i,j}\left(3\hat{\mu}_{i,j} - \hat{\upsilon}_{i,j}\right)\left(\hat{\Delta}_{i,j} - F^y_{i,j}\right) + \hat{\upsilon}_{i,j}\left(F^y_{i,j+1} - \hat{\Delta}_{i,j}\right)\left(7\hat{\mu}_{i,j} + \hat{\upsilon}_{i,j}\right)\right\} \big/ \hat{h}_j ,$$

$$U_{5,j} = 2\hat{\mu}_{i,j}^2 \left\{ \left(5\hat{\mu}_{i,j} + 2\hat{\upsilon}_{i,j}\right)\left(F_{i,j+1}^y - \hat{\Delta}_{i,j}\right) - 2\hat{\upsilon}_{i,j}\left(\hat{\Delta}_{i,j} - F_{i,j}^y\right) \right\} \Big/ \hat{h}_j ,$$
$$U_{6,j} = 2\hat{\upsilon}_{i,j}^2 \left\{ \left(\hat{\mu}_{i,j} + \hat{\upsilon}_{i,j}\right)\left(F_{i,j+1}^y - \hat{\Delta}_{i,j}\right) - \hat{\mu}_{i,j}\left(\hat{\Delta}_{i,j} - F_{i,j}^y\right) \right\} \Big/ \hat{h}_j ,$$

Similarly

$S^{(2)}\left(x_i, y\right) > 0$, if $U_{i,j}{}'s > 0, \quad i = 1, 2, \ldots, 6$ and $\hat{q}_{i,j}(\phi) > 0$

$\hat{q}_{i,j}(\phi) > 0$ if $\hat{\mu}_{i,j} > 0$, $\hat{\upsilon}_{i,j} > 0$ and $U_{i,j}{}'s > 0$, if

$$\hat{\mu}_{i,j} > 0,\ \hat{\upsilon}_{i,j} > 0,\ \hat{\mu}_{i,j} > \frac{\left(F_{i,j+1}^y - F_{i,j}^y\right)\hat{\upsilon}_{i,j}}{\left(\hat{\Delta}_{i,j} - F_{i,j}^y\right)} \text{ and } \hat{\mu}_{i,j} > \frac{\left(\hat{\Delta}_{i,j} - F_{i,j+1}^y\right)\hat{\upsilon}_{i,j}}{\left(\hat{\Delta}_{i,j} - F_{i,j}^y\right)}$$

$$S^{(2)}\left(x_{i+1}, y\right) = \frac{\sum_{i=1}^{6} W_{i,j}\phi^{i-1}\left(1-\phi\right)^{6-i}}{\left(\hat{q}_{i+1,j}\left(\phi\right)\right)^3} \tag{11}$$

where

$$W_{1,j} = 2\hat{\mu}_{i+1,j}^2 \left\{ \left(\hat{\mu}_{i+1,j} + \hat{\upsilon}_{i+1,j}\right)\left(\hat{\Delta}_{i+1,j} - F_{i+1,j}^y\right) - \hat{\upsilon}_{i+1,j}\left(F_{i+1,j+1}^y - \hat{\Delta}_{i+1,j}\right) \right\} \Big/ \hat{h}_j ,$$
$$W_{2,j} = 2\hat{\upsilon}_{i+1,j}^2 \left\{ \left(2\hat{\mu}_{i+1,j} + 5\hat{\upsilon}_{i+1,j}\right)\left(\hat{\Delta}_{i+1,j} - F_{i+1,j}^y\right) - 2\hat{\upsilon}_{i+1,j}\left(F_{i+1,j+1}^y - \hat{\Delta}_{i+1,j}\right) \right\} \Big/ \hat{h}_j ,$$
$$W_{3,j} = 2\hat{\mu}_{i+1,j} \left\{ \hat{\mu}_{i+1,j}\left(\hat{\mu}_{i+1,j} + 7\hat{\upsilon}_{i+1,j}\right)\left(\hat{\Delta}_{i+1,j} - F_{i+1,j}^y\right) + \hat{\upsilon}_{i+1,j}\left(F_{i+1,j+1}^y - \hat{\Delta}_{i+1,j}\right)\left(-\hat{\mu}_{i+1,j} + 3\hat{\upsilon}_{i+1,j}\right) \right\} \Big/ \hat{h}_j ,$$
$$W_{4,j} = 2\hat{\upsilon}_{i+1,j} \left\{ \hat{\mu}_{i+1,j}\left(3\hat{\mu}_{i+1,j} - \hat{\upsilon}_{i+1,j}\right)\left(\hat{\Delta}_{i+1,j} - F_{i+1,j}^y\right) + \hat{\upsilon}_{i+1,j}\left(F_{i+1,j+1}^y - \hat{\Delta}_{i+1,j}\right)\left(7\hat{\mu}_{i+1,j} + \hat{\upsilon}_{i+1,j}\right) \right\} \Big/ \hat{h}_j ,$$
$$W_{5,j} = 2\hat{\mu}_{i+1,j}^2 \left\{ \left(5\hat{\mu}_{i+1,j} + 2\hat{\upsilon}_{i+1,j}\right)\left(F_{i+1,j+1}^y - \hat{\Delta}_{i+1,j}\right) - 2\hat{\upsilon}_{i+1,j}\left(\hat{\Delta}_{i+1,j} - F_{i+1,j}^y\right) \right\} \Big/ \hat{h}_j ,$$
$$W_{6,j} = 2\hat{\upsilon}_{i+1,j}^2 \left\{ \left(\hat{\mu}_{i+1,j} + \hat{\upsilon}_{i+1,j}\right)\left(F_{i+1,j+1}^y - \hat{\Delta}_{i+1,j}\right) - \hat{\mu}_{i+1,j}\left(\hat{\Delta}_{i+1,j} - F_{i+1,j}^y\right) \right\} \Big/ \hat{h}_j ,$$

$S^{(2)}\left(x_{i+1}, y\right) > 0$, if $W_{i,j}{}'s > 0, \quad i = 1, 2, \ldots, 6$ and $\hat{q}_{i+1,j}(\phi) > 0$

$\hat{q}_{i+1,j}(\phi) > 0$ if $\hat{\mu}_{i+1,j} > 0$, $\hat{\upsilon}_{i+1,j} > 0$ and $W_{i,j}{}'s > 0$, if

$$\hat{\mu}_{i+1,j} > 0,\ \hat{\upsilon}_{i+1,j} > 0,\ \hat{\mu}_{i+1,j} > \frac{\left(F_{i+1,j+1}^y - F_{i+1,j}^y\right)\hat{\upsilon}_{i+1,j}}{\left(\hat{\Delta}_{i+1,j} - F_{i+1,j}^y\right)} \text{ and } \hat{\mu}_{i+1,j} > \frac{\left(\hat{\Delta}_{i+1,j} - F_{i+1,j+1}^y\right)\hat{\upsilon}_{i+1,j}}{\left(\hat{\Delta}_{i+1,j} - F_{i+1,j}^y\right)}.$$

All the above discussion can be summarized in the form of following theorem:

Theorem 4: The rational bi-cubic partially blended function defined in (3) preserves the shape of convex data in the view of convex surface, in each rectangular patch $I_{i,j}=\left[x_i,x_{i+1}\right]\times\left[y_j,y_{j+1}\right]$, if the shape parameters $\mu_{i,j},\upsilon_{i,j},\mu_{i,j+1},\upsilon_{i,j+1},\hat{\mu}_{i,j},\hat{\upsilon}_{i,j},\hat{\mu}_{i+1,j}$ and $\hat{\upsilon}_{i+1,j}$ satisfy the following conditions:

$$\upsilon_{i,j}>0,\ \upsilon_{i,j+1}>0,\ \hat{\upsilon}_{i,j}>0,\ \hat{\upsilon}_{i+1,j}>0,$$

$$\mu_{i,j}=\alpha_{i,j}+\max\left\{0,\ \frac{\left(F^x_{i+1,j}-F^x_{i,j}\right)\upsilon_{i,j}}{\left(\Delta_{i,j}-F^x_{i,j}\right)},\ \frac{\left(\Delta_{i,j}-F^x_{i+1,j}\right)\upsilon_{i,j}}{\left(\Delta_{i,j}-F^x_{i,j}\right)}\right\}$$

$$\mu_{i,j+1}=\beta_{i,j}+\max\left\{0,\ \frac{\left(F^x_{i+1,j+1}-F^x_{i,j+1}\right)\upsilon_{i,j+1}}{\left(\Delta_{i,j+1}-F^x_{i,j+1}\right)},\ \frac{\left(\Delta_{i,j+1}-F^x_{i+1,j+1}\right)\upsilon_{i,j+1}}{\left(\Delta_{i,j+1}-F^x_{i,j+1}\right)}\right\}$$

$$\hat{\mu}_{i,j}=\hat{\alpha}_{i,j}+\max\left\{0,\ \frac{\left(F^y_{i,j+1}-F^y_{i,j}\right)\hat{\upsilon}_{i,j}}{\left(\hat{\Delta}_{i,j}-F^y_{i,j}\right)},\ \frac{\left(\hat{\Delta}_{i,j}-F^y_{i,j+1}\right)\hat{\upsilon}_{i,j}}{\left(\hat{\Delta}_{i,j}-F^y_{i,j}\right)}\right\}$$

$$\hat{\mu}_{i+1,j}=\hat{\beta}_{i,j}+\max\left\{0,\ \frac{\left(F^y_{i+1,j+1}-F^y_{i+1,j}\right)\hat{\upsilon}_{i+1,j}}{\left(\hat{\Delta}_{i+1,j}-F^y_{i+1,j}\right)},\ \frac{\left(\hat{\Delta}_{i+1,j}-F^y_{i+1,j+1}\right)\hat{\upsilon}_{i+1,j}}{\left(\hat{\Delta}_{i+1,j}-F^y_{i+1,j}\right)}\right\},$$

where $\alpha_{i,j},\ \beta_{i,j},\ \hat{\alpha}_{i,j},\ \hat{\beta}_{i,j}>0$.

The above discussion can be summarized in the following algorithm for computation purposes:

Algorithm 2:

Step 1. Enter the $(n+1)\times(m+1)$ convex data points $\left(x_i,y_j,F_{i,j}\right), i=0,1,2,...,n;\ \ j=0,1,2,...,m.$

Step 2. Estimate the derivatives $F^x_{i,j},F^y_{i,j}$ and $F^{xy}_{i,j}$ at knots.

Step 3. Calculate the values of shape parameters $\mu_{i,j},\upsilon_{i,j},\mu_{i,j+1},\upsilon_{i,j+1},\hat{\mu}_{i,j},\hat{\upsilon}_{i,j},\hat{\mu}_{i+1,j}$ and $\hat{\upsilon}_{i+1,j}$ using Theorem 4.

Step 4. Substitute the values of $F_{i,j},\ F^x_{i,j},F^y_{i,j},F^{xy}_{i,j},\ \forall\, i=0,1,2,...,n;\ j=0,1,2,...,m$ and $\mu_{i,j},\ \upsilon_{i,j},\ \mu_{i,j+1},\ \upsilon_{i,j+1},\hat{\mu}_{i,j},\hat{\upsilon}_{i,j},\hat{\mu}_{i+1,j},\ \hat{\upsilon}_{i+1,j}\quad \forall\ i=0,1,2,...,n-1;\quad j=0,1,2,...,m-1$ in rational bi-cubic function (3) to obtain the convex rational bi-cubic function.

Table 3. A data set generated by $F_2\left(x,y\right)=x^4+y^2$.

y_j/x_i	-2	-1	0	1	2
-2	20	5	4	5	20
-1	17	2	1	2	17
0	16	1	0	1	16
1	17	2	1	2	17
2	20	5	4	5	20

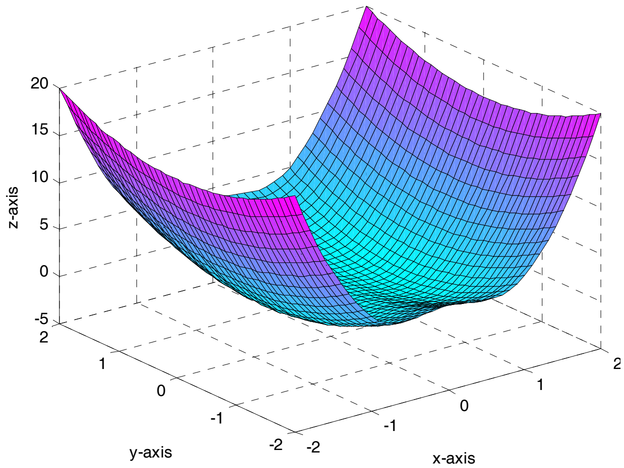

Figure 7. Bi-cubic Hermite Function

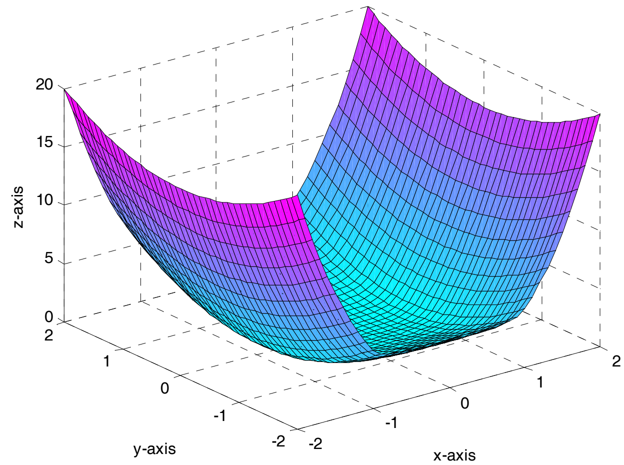

Figure 10. Convex rational bi-cubic Surface.

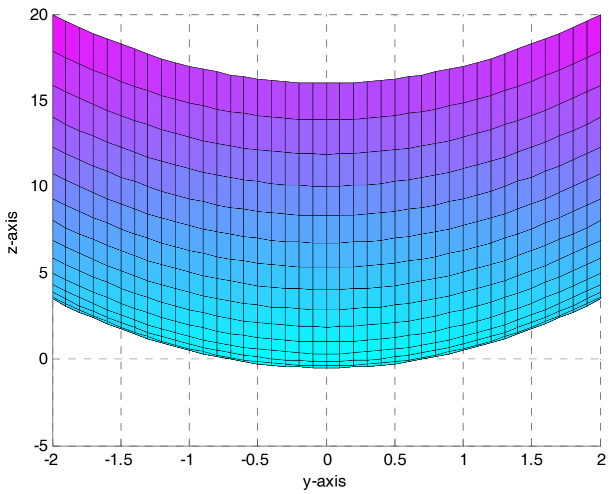

Figure 8. *yz*-view of Figure 7.

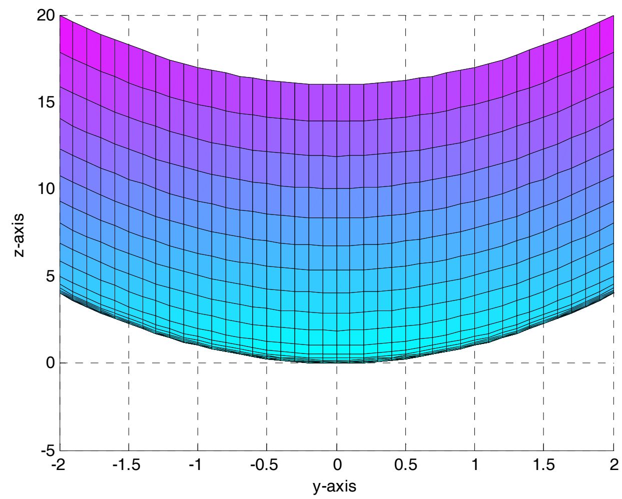

Figure 11. *yz*-view of Figure 10.

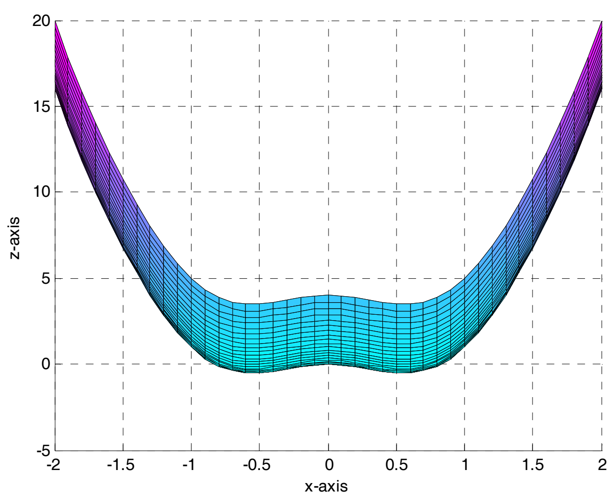

Figure 9. *xz*-view of Figure 7.

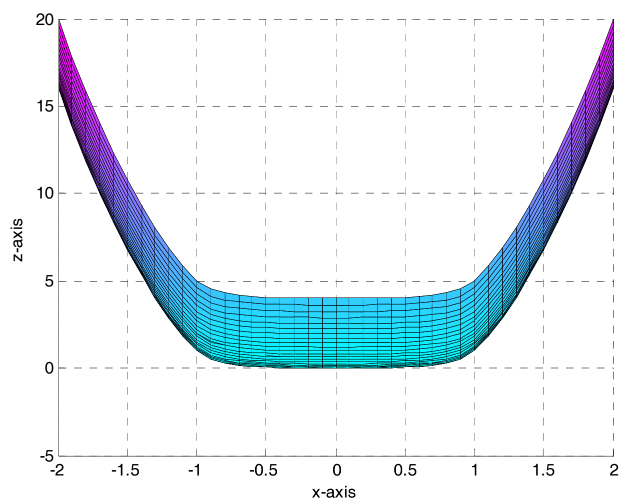

Figure 12. *xz*-view of Figure 10.

5.1. Demonstration:

A convex data set is taken in Table 3, which is generated by the function $F_2(x, y) = x^4 + y^2$, defined over the rectangular grid $[-2, 2] \times [-2, 2]$. Figure 7 is generated by using bi-cubic Hermite function, which interpolates the data points but does not preserve the shape of convex data. Figures 8 and 9 are the *yz*-view and *xz*-view of Figure 7 respectively. Figure 10 is generated by the convex rational bi-cubic function developed in Section 5 with $\upsilon_{i,j} = 5$, $\upsilon_{i,j+1} = 4$, $\hat{\upsilon}_{i,j} = 3$ and $\hat{\upsilon}_{i+1,j} = 2$. Figures 11 and 12 are the *yz*-view and *xz*-view of Figure 10 respectively. It can be observed that Figure 10 preserved the shape of data taken in Table 3.

Table 4. Numerical results of Figure 10.

(x_i, y_j)	$F_x(i, j)$	$F_y(i, j)$	$\mu_{i,j}$	$\mu_{i,j+1}$	$\hat{\mu}_{i,j}$	$\hat{\mu}_{i+1,j}$
(-2,-2)	-22	-4	5.0027	4.0032	3.0041	2.0051
(-2,-1)	-22	-2	5.0027	4.0032	3.0041	2.0051
(-2,0)	-22	0	5.0027	4.0032	3.0041	2.0051
(-2,1)	-22	2	5.0027	4.0032	3.0041	2.0051
(-2,2)	-22	4	5.0027	4.0032	3.0041	2.0051
(-1,-2)	-8	-4	5.0027	4.0032	3.0041	2.0051
(-1,-1)	-8	-2	5.0027	4.0032	3.0041	2.0051
(-1,0)	-8	0	5.0027	4.0032	3.0041	2.0051
(-1,1)	-8	2	5.0027	4.0032	3.0041	2.0051
(-1,2)	-8	4	5.0027	4.0032	3.0041	2.0051
(0,-2)	0	-4	5.0027	4.0032	3.0041	2.0051
(0,-1)	0	-2	5.0027	4.0032	3.0041	2.0051
(0,0)	0	0	5.0027	4.0032	3.0041	2.0051
(0,1)	0	2	5.0027	4.0032	3.0041	2.0051
(0,2)	0	4	5.0027	4.0032	3.0041	2.0051
(1,-2)	8	-4	5.0027	4.0032	3.0041	2.0051
(1,-1)	8	-2	5.0027	4.0032	3.0041	2.0051
(1,0)	8	0	5.0027	4.0032	3.0041	2.0051
(1,1)	8	2	5.0027	4.0032	3.0041	2.0051
(1,2)	8	4	5.0027	4.0032	3.0041	2.0051
(2,-2)	22	-4	5.0027	4.0032	3.0041	2.0051
(2,-1)	22	-2	5.0027	4.0032	3.0041	2.0051
(2,0)	22	0	5.0027	4.0032	3.0041	2.0051
(2,1)	22	2	5.0027	4.0032	3.0041	2.0051
(2,2)	22	4	5.0027	4.0032	3.0041	2.0051

The numerical results corresponding to the surface in Figure 10, for different parameters, are shown in Table 4. All the values in Table 4 are truncated up to four decimal places.

6. Conclusion

A rational bi-cubic partially blended function (bi-cubic/bi-quadratic) is introduced, to preserve the shape of positive and convex data. Eight free parameters are attached in the description of rational bi-cubic partially blended function. Simple data dependent constraints are derived on free parameters to preserve the shape of positive and convex data in the view of positive and convex surfaces respectively. Developed schemes work for both equally and unequally spaced data. In the developed schemes there is no constraint on derivatives, they are equally useful for the data with or without derivatives. Developed schemes are local and C^1.

References

[1] M. R. Asim & K. W. Brodlie, Curve drawing subject to positivity and more general constraints, *Computers and Graphics*, **27**, (2003), 469-485.

[2] K. W. Brodlie, M. R. Asim & K. Unsworth, Constrained visualization using the Shepard interpolation family, *Computer Graphics Forum* **24(4),** (2005), 809-820.

[3] K. Brodlie, P. Mashwama & S. Butt, Visualization of surface data to preserve positivity and other simple constraints, *Computers and Graphics*, **19(9)**, (1995), 585-594.

[4] G. Casciola & L. Romani, Rational interpolants with tension parameters, Curves and Surface Design, *Tom Lyche, Marie-Laurence Mazure and Larry L. Schumaker(eds.)*, (2003), 41-50.

[5] Q. Duan, Y. Zhang & E. H. Twizell, A bivariate rational interpolation and the properties, *Applied Mathematics and Computation*, **179**, (2006), 190-199.

[6] B. Fangxum, S. Qinghua & Q. Duan, A bivariate blending interpolator based on function values and its applications, *Journal of Computational Information Science*, **6(10)**, (2010), 3381-3389.

[7] N. Fujisawa, K. Brown, Y. Nakayama, J. Hyatt & T. Corby, Visualization of scientific arts and some examples of applications, *Journal of Visualization*, **11(4)**, (2008), 387-394.

[8] M. Z. Hussain & M. Hussain, Visualization of 3D data preserving convexity, *Journal of Applied Mathematics and Computing*, **23(2)**, (2007), 397-410.

[9] M. Z. Hussain, M. Hussain & S. S. Tahira, Shape Preserving Convex Surface Data Visualization using rational bi-quartic function, *European Journal of Scientific Research*, **21(2),** (2008), 319-327.

[10] M. Z. Hussain, M. Sarfraz, & S. S. Tahira, Shape Preserving Rational Cubic Spline for Positive and Convex Data, accepted in *Egyptian Informatics Journal*, (2011).

[11] A. Kouibia & M. Pasadas, Approximation by interpolating variational splines, *Journal of Computational and Applied Mathematics*, **218,** (2008), 342-349.

[12] A. R. M. Piah, T. N. T. Goodman & K. Unsworth, Positivity preserving scattered data interpolation, in: *Proceedings of the 11th IMA Mathematics of Surfaces Conference, Loughborough, UK, September 5-7*, (2005) 336-349.

[13] R. J. Renka, Interpolation of scattered data with a C^1 convexity preserving surface, *ACM Transactions on Mathematical Software*, **30(2)**, (2004), 200-211.

[14] M. Sarfraz, M. Z. Hussain & A. Nisar, Positive data modeling using spline function, *Applied Mathematics and Computation*, **216**, (2010), 2036-2049.

[15] Wang & J. Tan, Shape preserving piecewise rational biquartic surfaces, *Journal of Information and Computational Sciences*, **3(2)**, (2006), 295-302.

[16] Y. Zhang, Q. Duan & E. H. Twizell, Convexity control of a bivariate rational interpolating spline surfaces, *Computers and Graphics*, **31**, (2007), 679-689.